Low-Frequency Small-Signal Modeling of Interconnected AC Microgrids

Naderi, Mobin; Shafiee, Qobad; Bevrani, Hassan ; Blaabjerg, Frede

Published in:
I E E E Transactions on Power Systems

DOI (link to publication from Publisher):
10.1109/TPWRS.2020.3040804

Publication date:
2021

Document Version
Accepted author manuscript, peer reviewed version

This article has been accepted for publication in a future issue of this journal, but has not been fully edited. Content may change prior to final publication. Citation information: DOI 10.1109/TPWRS.2020.3040804, IEEE Transactions on Power Systems

Low-Frequency Small-Signal Modeling of Interconnected AC Microgrids

Mobin Naderi, *Student Member, IEEE,* Qobad Shafiee, *Senior Member, IEEE,* Frede Blaabjerg, *Fellow, IEEE* and Hassan Bevrani, *Senior Member, IEEE,*

***Abstract*—As a solution for optimized, reliable and flexible operation of distribution systems, multiple AC microgrids can be interconnected. In this paper, a low-order low-frequency small-signal model is proposed for large-scale interconnected AC microgrids in order to analyze stability and dynamics as well as synthesize high-level controllers, e.g. inter-microgrid power flow controller. A sensitivity analysis-based technique is introduced to find significant modules of fully inverter-based AC microgrids for preserving the dominant low-frequency modes. The low-order model of AC microgrids including both droop-based and PQ-controlled distributed generation units is obtained by removing insignificant modules of the detailed model and reconfiguring the significant modules. The concept of virtual swing equation and the aggregation modeling method are employed to achieve a single-order model from the low-order model for each AC microgrid with any number of sources. The analysis and synthesis of the large-scale interconnected microgrids can easily be done using the proposed single-order model. The frequency analysis and control of three interconnected AC microgrids are presented as a case study, which leads to introducing the inter-microgrid oscillatory modes.**

***Index Terms*—Aggregation method, dominant low-frequency modes, interconnected AC microgrids, sensitivity analysis, simplified model, virtual swing equation.**

I. Introduction

SINCE the distributed generation units (DGUs) have limitations and the loads are dispersed, they have been integrated within the concept of microgrid (MG). As a solution for accessing more flexibility, reliability and sustainability, the interconnected microgrids (IMGs) have recently been introduced. Both AC and DC MGs and different interconnections among them are taken into account in terms of optimal operation, control and stability analysis [1]–[10]. However, the AC IMGs have been more favorable due to available AC distribution systems and their challenges. As the first step, the challenges of stability and control of IMGs should be solved, especially when they lead to large-scale nested systems. In such systems, low-order models focusing on the slow dynamic modes are more interesting for main modules, i.e. AC MGs. Hence, modeling, stability analysis, and high-level controller design of several IMGs with different structures are facilitated.

Generally speaking, the modeling methods are divided into small-signal and large-signal types. Although the large-signal methods are based on nonlinear equations, linearized equations around an equilibrium point are utilized for the small-signal modeling. On the other hand, the modeling method types are dependent on the kind of studied dynamics. For MG dynamics, the phenomena can be classified into four groups, i.e. very fast, fast/medium, slow and very slow phenomena. Harmonic studies, voltage/frequency control, demand response, and power management are examples, respectively [11]. For each phenomena group, different types of modeling methods with their requirements are needed to model corresponding dynamics, which in turn can be categorized into detailed and simplified modeling types. A detailed modeling method for fast/medium MG dynamics has been presented in [12], which leads to a large range of frequencies to be assessed. In contrast, the simplified models are addressed focusing on a special frequency range, particularly low frequencies [13]–[17].

The simplified modeling methods can be organized into three clusters, i.e. model-based, module-based, and measurement-based simplification approaches. In the first cluster, the detailed model should be obtained for each studied system, then its order can be reduced using aggregation and perturbation methods [18]. The perturbation methods including regular (e.g., [19]) and singular (e.g., [13]–[17], [20]) types are often used in the MG dynamic studies. The second cluster tries to find the simplified model without calculating the detailed model. The dominant modules in the desired dynamics are preserved and the other are removed according to the knowledge of the system [6], [21]. Methods of the third cluster benefit from the measured data and system identification techniques, e.g. fast Fourier transform, Prony analysis [22], [23], discrete wavelet transform [24] and vector fitting technique [25]. Artificial-intelligence modeling techniques are also a group of the measurement-based methods [26], [27].

The AC MGs can be interconnected via circuit breakers [6], [20], [21], [28], static switches [3] or back-to-back converters [4], [5], [29]. The first case is often of interest since it is economic. Modeling of such AC IMGs is based on modeling of the main modules, i.e. individual AC MGs, where interlinking lines have a simple model and the circuit breakers can be neglected. Most of the literature have concentrated on the AC MG with fully inverter-based DGUs [13]–[17], [21], [30], [31], which is also the basic structure in this paper. The simplification procedure can be of two steps,

M. Naderi, Q. Shafiee, and H. Bevrani are with the Smart/Micro Grids Research Center (SMGRC), University of Kurdistan, Sanandaj, Iran, P.C.: 66177-15175. E-mail: (m.naderi@eng.uok.ac.ir, q.shafiee@uok.ac.ir, and bevrani@eng.uok.ac.ir), website: https://smgrc.uok.ac.ir/.

F. Blaabjerg is with Department of Energy Technology, Aalborg University, Aalborg, DK, 9220, Denmark. E-mail: (fbl@et.aau.dk).

This paper was supported by the Reliable Power Electronic based Power System (REPEPS) project at the Department of Energy Technology, Aalborg University, which is a part of the Villum Investigator Program (grant no. 25920) funded by the Villum Foundation.

This article has been accepted for publication in a future issue of this journal, but has not been fully edited. Content may change prior to final publication. Citation information: DOI 10.1109/TPWRS.2020.3040804, IEEE Transactions on Power Systems

comprising of simplifying the electrical network and reducing the order of inverters individually. The first step have usually been accomplished using Kron reduction method [13], [17], [21]. However, non-simplified networks [15], [16], [30] and simple networks with single point of common coupling (PCC) [14], [31] are also considered in the literature. In addition, a reduced-order model based on the modified Krylov subspace method is developed for active distribution networks [32]. Regarding the second step, several reduced-order models have been presented for inverters consisting of eighth-order [15], fifth-order [13], third-order [13], [16], [31], [33], second-order [17] and single-order [13], [14]. In [13], [14], [17], [20] the coupling line is included in the inverter model as a significant module in forming the dominant modes.

In an order-reducing process, mostly, the fast dynamic modes are removed and the slow dominant modes are preserved using the balanced Residualization realization (singular perturbation theory) [13]–[17], [20]. Nevertheless, in [19], the balanced Truncation realization (regular perturbation theory) is used in order to achieve a second-order model of PQ-controlled grid-feeding inverters. Furthermore, in [21], the aggregation methods and quasi-static equations are employed for IMGs to map all similar modules in each AC MG, e.g. droop-based DGUs have one equivalent module. In this method, each module model has not been simplified. Another study on IMGs focuses on the stability assessment through finding the critical clusters of DGUs, which has employed the singular perturbation method [20].

In this paper, a reduced-order low-frequency model is proposed for circuit breaker-coupled AC IMGs with fully inverter-based DGUs employing both perturbation and aggregation methods. The low-order IMG model with the method of calculating the main parameters, i.e. the virtual moment of inertia and the damping coefficient of MGs, is the main paper novelty. Compared with existing works, the contribution of this paper can be clarified as follows:

- Unlike existing works [17], [20], the proposed simplification method is not just based on the participation matrix. Here, a family of AC MGs are considered with different ranges of parameters using the sensitivity analysis. Therefore, the significant modules for preserving the dominant low-frequency modes (DLFMs) can be found for all possible amounts of parameters. In other words, the method is robust against the parameter changes.
- The proposed simplification method is a module-based scalable one. Here, the detailed model is used just for the searching process of the significant modules. After finding these significant MG modules on the DLFMs, any number of the preserved modules can be interconnected to form any desired MG structure.
- The simplification starts by using singular and regular perturbation methods regarding modules dynamics, and then it will be completed by aggregating the oscillatory DLFMs into a couple of complex conjugate eigenvalues. It leads to a second-order model for AC MGs.
- The concept of virtual swing equation is introduced to achieve a single-order model for autonomous AC MGs with reasonable and calculated values for virtual inertia and damping coefficient. In [34], a single-order model is considered for AC MGs with both inertia-less and rotational DGUs, which in fact shows the real inertia of the rotational units and neglects the inertia-less units. A similar system is represented in [35], where the single-order model is calculated based on a Prony measurement-based method. In [36], [37], the amounts of equivalent inertia for the single-order model of AC MGs is not reasonable, because they have just been assumed, but not been calculated according to the real AC MGs data.
- The single-order frequency model of AC MGs is able to be used in modeling the large-scale IMGs, stability analysis and also high-level controller design. While, high and medium-order models presented in [15], [17], [20], [21] are more hard to be employed in such studies.
- The oscillatory inter-microgrid modes are also addressed, which are not already known in the literature and can be of interest in the studies of IMG stability analysis and load-frequency control synthesis.

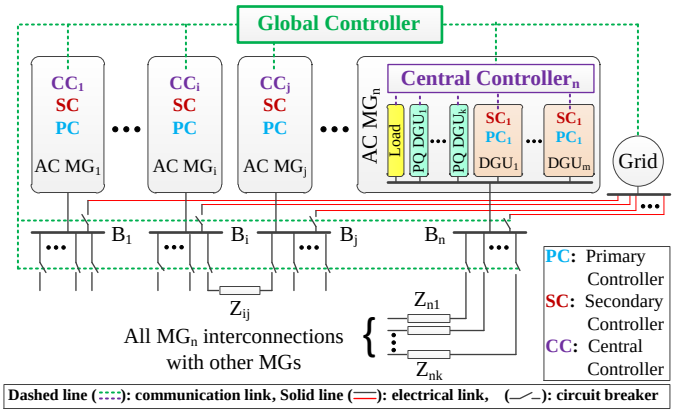

Fig. 1. General structure of interconnected AC MGs via circuit breakers, and tie lines under the four-level control architecture.

The rest of this paper is arranged as follows. An overview of the control and detailed modeling of IMGs is provided in Section II. The simplified low-frequency model and the single-order model of individual AC MGs are addressed in Sections III and IV, respectively. As an application of the proposed low-order model, a secondary frequency control of three IMGs and the simulation results are presented in Sections V and VI, respectively. Finally, the paper is concluded in Section VII.

II. Requirements of Interconnected Microgrids

A general structure of interconnected AC MGs via circuit breakers and AC tie-lines is shown in Fig. 1. Each MG may have different configuration with any number of DGUs and loads and it is assumed to be able to connect to other MGs and main grid through a PCC, e.g. B_n for MG_n. Both droop-based and PQ-controlled DGUs are considered in the AC MGs. The droop-based DGUs can participate in voltage/frequency control and power sharing. However, the PQ-controlled DGUs try to maximize the production of renewable units and cannot contribute to droop-based DGU duties.

A multi time-scale control is required for a coordinated control among IMGs, as well as controllable units within each AC MG. Here, four-level hierarchical control [11] is employed,

This article has been accepted for publication in a future issue of this journal, but has not been fully edited. Content may change prior to final publication. Citation information: DOI 10.1109/TPWRS.2020.3040804, IEEE Transactions on Power Systems

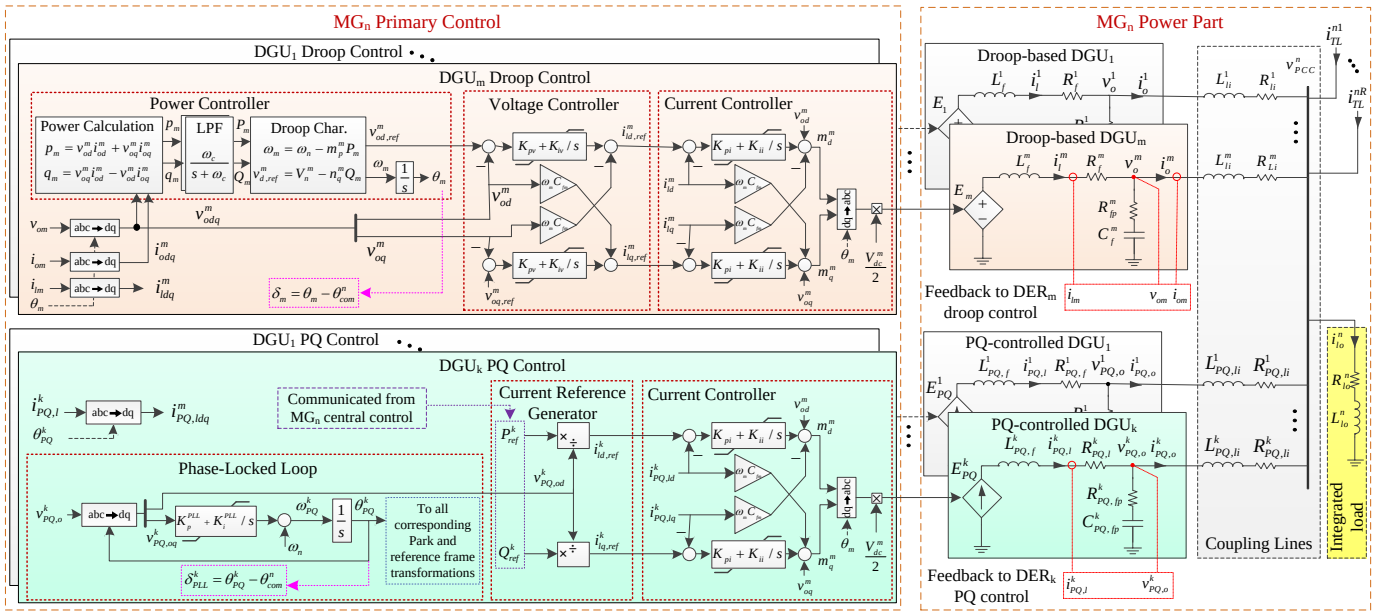

Fig. 2. The structure of the studied autonomous AC microgrids including both droop-based and PQ-controlled DGUs, and considering a simplified network into coupling DGU lines and also an integrated load.

containing the primary, secondary, central and global control levels. Voltage/frequency stability, primary active/reactive power sharing, and current limiting are the main purposes of the primary control (PC). Power sharing improvement and voltage/frequency restoration to the nominal values are accomplished by the secondary control (SC) [38]. The central control (CC) coordinates the controllable DGUs and loads for power balance and enhances the supervisory activities, e.g. islanding detection and emergency control [11]. At last, the global control apply the optimal power flow among IMGs themselves and the main grid.

Interlinking circuit breakers are assumed to switch as quick as they are neglected in the proposed slow dynamic modeling. Therefore, the main modules of the IMGs needed to be modeled are the AC individual MGs and the tie-lines as shown by Z impedances in Fig. 1.

A. Detailed Microgrid Model

Fig. 2 shows the general structure of the studied AC MG comprising m droop-based and k PQ-controlled DGUs using the primary control. Two assumptions are considered in relation to the power part: 1) the structure of single-PCC is selected [14], [31], where all DGUs are connected by the coupling lines, 2) all loads including local DGU loads and common loads are integrated into one equivalent load at the PCC. Here, the focus is not on the power part simplification since it is not important for finding the slow dynamics except the coupling lines [17], which are included in the modeling. However, for more generalizing of MG structure, one can consider a multiple-PCC network structure or different load types, which each idea is able to be taken into account in future works and dealt with the corresponding challenges, i.e. the impacts of the MG structure and the load types on the IMG dynamic modeling and stability.

The authors have previously presented an interconnection modeling method [29], which is employed here for finding the detailed model of autonomous AC MGs. In this method, state space representation of each module/component of an AC MG is separately calculated as presented in Section II-B. Then all the interconnections among any number of modules are easily realized using the corresponding functions of the Robust Control Toolbox/MATLAB. Fig. 3 shows the process of the interconnection method for AC MGs with more details.

B. Main Microgrid Modules

Modeling of each module is realized by finding its state space representation as follows

$$\dot{X}_m = A_m X_m + B_m U_m, \tag{1a}$$

$$Y_m = C_m X_m + D_m U_m, \tag{1b}$$

where X_m, U_m, and Y_m are the state, input, and output vectors of the module and they are presented in Table I for all modules. The matrices A_m, B_m, C_m, and D_m can easily be found by considering the vectors expressed in Table I and using the circuit and control laws in Fig. 2. Furthermore, they are given in [29] in detail. Note that the modeling of tie-lines is similar to the coupling line modeling shown in Table I.

III. Simplified Low-Frequency Model

The purpose of this Section is to present a systematic method to find a low-order model of autonomous AC MGs containing only slow modes. In fact, the significant modules for finding the DLFMs should be preserved and the insignificant modules must be removed from the detailed model. Reconfiguring the maintained modules completes the simplification method.

The participation matrix is a well-known tool for recognizing the correlation between eigenvalues/modes and state variables of the modules. However, its array amounts is correlated to the system parameters. Therefore, the results are not acceptable for different amounts of AC MG parameters.

This article has been accepted for publication in a future issue of this journal, but has not been fully edited. Content may change prior to final publication. Citation information: DOI 10.1109/TPWRS.2020.3040804, IEEE Transactions on Power Systems

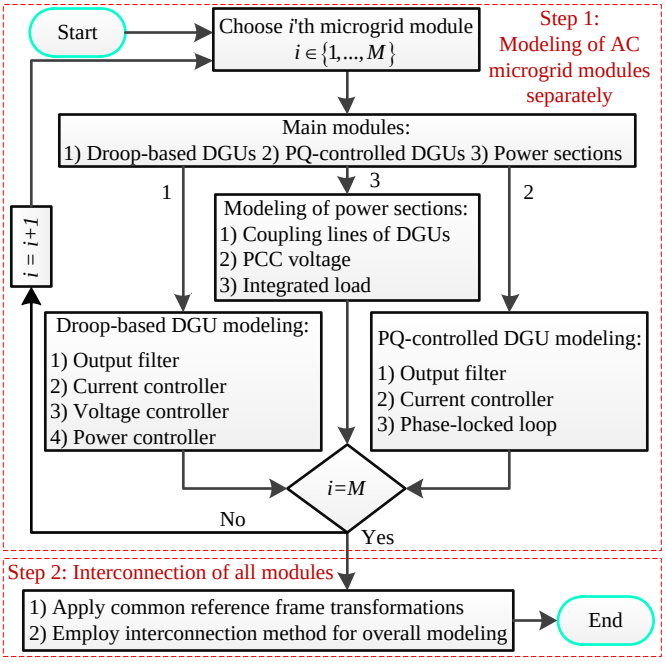

Fig. 3. Process of the interconnection modeling method [29] for finding the detailed model of autonomous AC microgrids in two generic steps.

TABLE I. VARIABLES, INPUT, AND OUTPUT VECTORS OF STATE SPACE REPRESENTATION OF MICROGRID MODULES RELATED TO FIG. 2

Module	State variables (X_m)	Inputs (U_m)	Outputs (Y_m)
Droop-based DGU$_m$			
Output filter	$[i_l^m\ v_o^m]^T$	$[E_m\ \omega_{com}\ i_o^m]^T$	$= X_m$
Current controller	Integrator outputs	$[i_l^m\ v_o^m\ i_{l,ref}^m]^T$	E_m
Voltage controller	Integrator outputs	$[v_o^m\ v_{o,ref}^m]^T$	$i_{l,ref}^m$
Power controller	$[\delta_m\ P_m\ Q_m]^T$	$[v_o^m\ i_o^m\ \omega_{com}]^T$	[a]
PQ-controlled DGU$_k$			
Output filter	$[i_{PQ,l}^k\ v_{PQ,o}^k]^T$	[b]	$= X_m$
Current controller	Integrator outputs	$[i_{PQ,l}^k\ v_{PQ,o}^k]^T$	$E_{PQ,k}$
PLL	Integrator outputs	$[v_{PQ,o}^k\ \omega_{com}]^T$	δ_{PLL}
Power sections			
Coupling lines[c]	$i_{PQ,o}^k$	[d]	$= X_m$
PCC voltage	-	[e]	v_{PCC}^n
Integrated load	i_{lo}^n	$[v_{PCC}^n\ \omega_{com}]^T$	$= X_m$

[a] $[\ \omega_m\ v_{o,ref}^m\ \delta_m]^T$, [b] $[E_{PQ}^k\ \omega_{com}\ i_{PQ,o}^k]^T$, [d] $[v_{PCC}^n\ v_{PQ,o}^k\ \omega_{com}]^T$
[c] For instance, DGU$_k$, [e] Currents of coupling lines, tie-lines and load

In fact, the participation matrix is not enough to specify the important state variables (modules) for finding the DLFMs when a family of autonomous AC MGs are considered, which is formed by changing the parameters in acceptable ranges. Hence, the sensitivity analysis is employed to analyze such MGs family.

A. Sensitivity Analysis-Based Simplification Method

Fig. 4 shows how the sensitivity analysis is used for sifting out the significant modules for preserving the DLFMs from the insignificant ones. The detailed model is the start point in order to be sure that all modules are checked. For each module, all its parameters are changed within acceptable ranges. The criterion for preserving a module is a minimum sensitivity (ε) of at least one of the DLFMs to at least one of its parameters:

$$d\lambda_{DLFM}/dp_k^i > \varepsilon, \tag{2}$$

where p_k^i is k'th parameter of i'th module. The variation of real value, imaginary value, damping ratio, or a combination of them for each eigenvalue can be selected to realize (2), i.e. recognizing the eigenvalue locus sensitivity to the parameter changes. Here, (2) is realized for oscillatory modes as follows

$$\Delta f > \Delta f_{Tr}, \tag{3a}$$
$$\Delta \zeta > \Delta \zeta_{Tr}, \tag{3b}$$

where, Δf and $\Delta \zeta$ are the frequency and damping ratio variations of the DLFM due to changing p_k^i. Δf_{Tr} and $\Delta \zeta_{Tr}$ are the threshold values specifying the ease/hardness of fulfilling (2). However, the absolute real value variation ($\Delta \sigma$) is considered for the non-oscillatory modes as follows

$$\Delta \sigma > \Delta \sigma_{Tr}. \tag{4}$$

Δf_{Tr}, $\Delta \zeta_{Tr}$, and $\Delta \sigma_{Tr}$ are selected as 0.1 of the average frequency of the DLFMs such that $f_{DLFM} > 0$, 0.1 of the maximum damping ratio i.e. 1, and 0.1 of the margin between dominant and non-dominant modes, respectively. Finally, If the sensitive parameter set of i'th module (SP_i) is null, its states should be removed. Otherwise, they are preserved.

Fig. 5 shows the sensitivity analysis results typically for two modules including the power controller (Fig. 5(a)) and output filter (Fig. 5(b)) of a droop-based DGU in an MG with two droop-based DGUs. The vertical blue line shows the margin between dominant and non-dominant modes. The radial lines determine margins for recognizing (3b). Obviously, the DLFMs are sensitive to the power controller parameters, i.e. $\omega - P$ droop gain (m_p) and $V - Q$ droop gain (n_q), but not to the DER output filter parameters, i.e. filter capacitance (C_f) and inductance (L_f). In addition, the sensitivity analysis is done for two different X/R ratio of the DER coupling line, i.e. $X/R = 0.63$ and $X/R = 1.26$.

Employing the sensitivity analysis-based sifting method, one can classify the modules into two groups: 1) the significant modules for preserving the DLFMs including droop-based DGU power controller and coupling line, and PQ-controlled DGU current controller and PLL, and 2) insignificant modules comprising all other modules of the detailed model presented in Table I.

B. Removing/Reconfiguration Process of Modules

Note that all of the insignificant modules for preserving the DLFMs cannot be removed using the regular perturbation method. It is due to the inevitable effects of such modules in the solving process of the set of governing MG equations. Thus at least, their static model should be preserved, which can be found using the singular perturbation method. To this end, Consider the state space representation of a module with insignificant dynamics (X_{ID}) as

$$\varepsilon \dot{X}_{ID} = A_{ID}X_{ID} + B_{ID}U_{ID}, \tag{5a}$$
$$Y_{ID} = C_{ID}X_{ID} + D_{ID}U_{ID}, \tag{5b}$$

where U_{ID} and Y_{ID} are the input and output vectors and A_{ID}, B_{ID}, C_{ID}, and D_{ID} are the corresponding matrices with

This article has been accepted for publication in a future issue of this journal, but has not been fully edited. Content may change prior to final publication. Citation information: DOI 10.1109/TPWRS.2020.3040804, IEEE Transactions on Power Systems

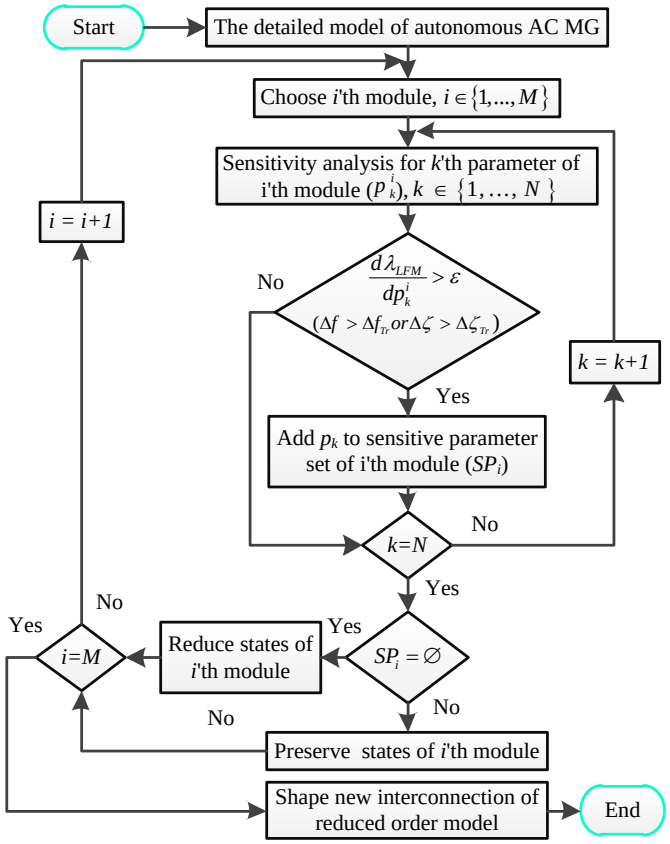

Fig. 4. Sensitivity analysis-based simplification flowchart for a family of autonomous AC microgrids via changing the parameters in the analysis.

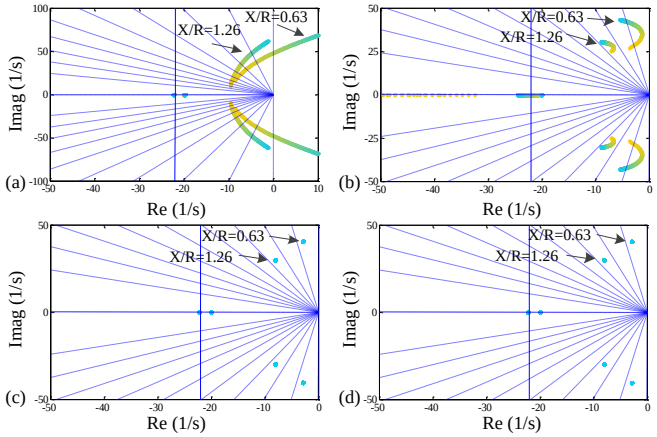

Fig. 5. Sensitivity analysis results of dominant low-frequency modes typically for droop-based DGU power controller parameters: (a) $0.001\% < m_p < 0.02\%$, (b) $0.01\% < n_q < 0.2\%$, and output filter parameters: (c) 0.3 mH$< L_f <$6.4 mH, (d) 3 $\mu F < C_f < 60\mu F$ (from yellow to blue).

appropriate sizes. Since all of the dynamics are insignificant, if $\varepsilon \to 0$ and A_{ID} is nonsingular, one can consider $\dot{X}_{ID} \to 0$ and replace X_{ID} from (5a) into (5b) in order to find the static model as follows

$$Y_{ID} = (D_{ID} - C_{ID}A_{ID}^{-1}B_{ID})U_{ID}. \tag{6}$$

The dynamics of the output filter and coupling line of PQ-controlled DGUs as well as the integrated load are deleted from the simplified model using this method and their static models are used.

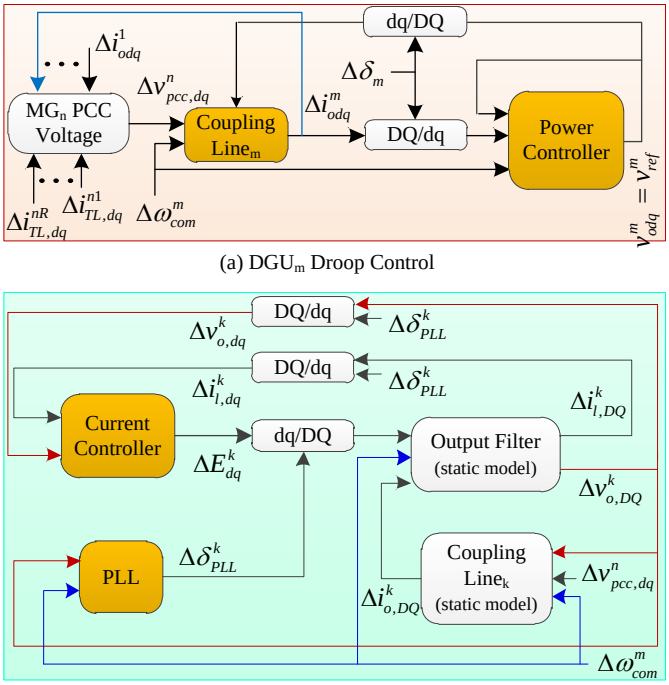

Fig. 6. Reconfiguration of DGU interconnections after removing insignificant modules for preserving the dominant low-frequency modes: (a) DGU$_m$ droop control, (b) DGU$_k$ PQ control.

Reconfiguration of the dynamic and static models of the preserved modules is shown in Fig. 6. The droop-based DGU$_m$ including the power controller and the common reference frame transformations (DQ/dq and dq/DQ) with the coupling line and PCC voltage are restructured as shown in Fig. 6(a). Since the dynamics of the current and voltage controllers are fast and can be removed, the input of the voltage controller v^m_{odq} will be equal to the output of the current controller v^m_{ref}. The structure of the simplified model of PQ-controlled DGU$_k$ can be obtained by replacing the static models of the output filter and coupling line as shown in Fig. 6(b).

In the representation of singular perturbation, the dynamics of compound modules such as droop-based DGU$_m$ or PQ-controlled DGU$_k$ can be divided into fast dynamics (X_{FD}) and slow dynamics (X_{SD}), which their relationship is as

$$\varepsilon\dot{X}_{FD} = A_{11}X_{FD} + A_{12}X_{SD}, \tag{7a}$$

$$\dot{X}_{SD} = A_{21}X_{FD} + A_{22}X_{SD}, \tag{7b}$$

where A_{11}, A_{12}, A_{21}, and A_{22} are the sub-matrices of the compound module state matrix. If $\varepsilon \to 0$ and A_{22} is nonsingular, by replacing X_{FD} from (7a) to (7b), the dynamic modes of the simplified module model are approximated as follows

$$\dot{X}_{SD} = (A_{22} - A_{21}A_{11}^{-1}A_{12})X_{SD}. \tag{8}$$

C. Validation of the Proposed Simplified Model

1) DLFMs Comparison of the Detailed and Proposed Models: In order to validate the proposed simplified model for autonomous AC MGs, the DLFMs are compared to DLFMs of the detailed model [12]. Figs. 7(a) and 7(b) show a comparison for an MG with two droop-based and one PQ-controlled DGUs

This article has been accepted for publication in a future issue of this journal, but has not been fully edited. Content may change prior to final publication. Citation information: DOI 10.1109/TPWRS.2020.3040804, IEEE Transactions on Power Systems

TABLE II. STATE VARIABLES OF THE COMPARED MODELS IN FIG. 8

Model	State variables	Ref.
M1	$\Delta\delta, \Delta P, \Delta Q, \Delta v_{odq}, \Delta i_{ldq}, \Delta i_{odq}$, CCIO[a], VCIO[b]	[12]
M2	Droop-based DGU: $\Delta\delta, \Delta P, \Delta Q, \Delta i_{odq}$ PQ-controlled DGU: $\Delta\delta_{PLL}$, CCIO, PLLIO[c]	Sec. III
M3	$\Delta\delta, \Delta P, \Delta Q, \Delta i_{odq}$	[13]
M4	$\Delta\delta, \Delta P, \Delta i_{odq}$	[17]
M5	$\Delta\delta, \Delta\omega, \Delta V_{od}$	[16]

[a] current controller integrator outputs, [b] voltage controller integrator outputs, [c] PLL integrator output

and another MG with four droop-based DGUs, respectively. The error can be calculated for each eigenvalue using the relative error percentage, which is 2.3 % in the worst case. In Fig. 7(a), the dynamic mode in Group (1) is the inter-inverter mode [17] expressing the interaction between the two droop-based DGUs. Note that the common reference frame is based on the frequency for one of the DGUs, e.g. the first droop-based DGU, which is named the base DGU in this paper. The dynamic mode in Group (2) shows the interaction between the single PQ-controlled DGU and the base DGU. An important fact is that the DLFMs, which show the interaction among DGUs are complex conjugates (oscillatory). In Fig. 7(b), there exist three oscillatory DLFMs showing the interaction between each droop-based DGU and the base DGU.

The two case studies indicate an oscillatory DLFM emulating the interaction between each DGU and the base DGU within the MGs. It is noteworthy that the result is generalized for droop-based DGUs in the studied family of AC MGs with any number of DGUs. Furthermore, the result is applicable for MGs with different power network structures [17]. Nevertheless, the oscillatory DLFMs expressing the interaction between PQ-controlled DGUs and the base DGU are limited to a relatively large subset of the studied MG family. Outside the specific parameter range, the oscillatory DLFMs will be transformed into two non-oscillatory modes. Here, the parameters of PQ-controlled DGUs are considered to be within the range causing the oscillatory DLFMs. The parameter ranges can easily be obtained via sensitivity analysis.

2) The Oscillatory DLFM Comparison of the Existing and Proposed Simplified Models: A sensitivity analysis is provided in Fig. 8 to compare the proposed simplified model with existing simplified models, which are usually named by the model order of each inverter belonged to each DGU. The simplified models includes a 5th-order model [13], a 4th-order model [17], and a 3rd-order model [16], which their preserved state variables are shown in Table II Moreover, the detailed model [12] is considered to be the reference model. An MG with two droop-based DGUs is considered. The oscillatory DLFM is of interest to be compared and non-dominant dynamic modes are not shown. For low values of m_p the proposed model has a higher accuracy due to its more similar behaviour to the detailed model behaviour. Generally, the proposed model shows almost a similar behaviour to the 5th-order model behaviour to the m_p changes. It is more accurate than the 4th-order and 3rd-order models. However, all the reduced-order models have lower tendency to be unstable by increasing m_p than the detailed model.

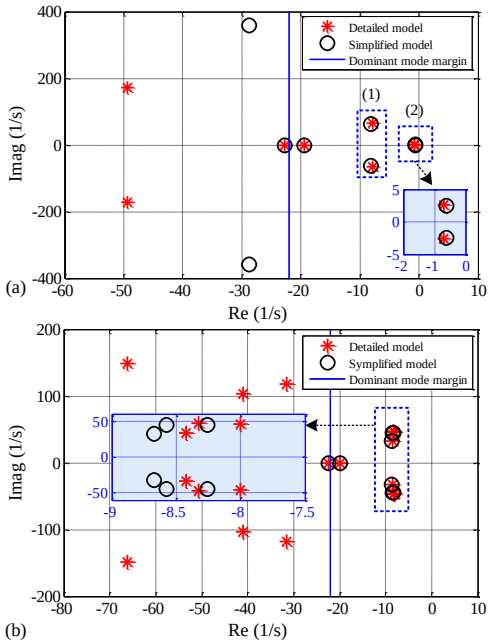

Fig. 7. The simplified model validation by comparing to the detailed model presented in [12]: (a) a microgrid with two droop-based and one PQ-controlled DGUs, (b) a microgrid with four droop-based DGUs.

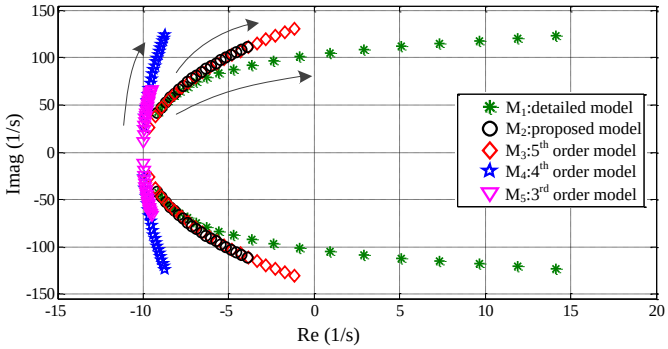

Fig. 8. The Oscillatory DLFM Comparison among the proposed model, existing simplified models and the detailed model by sensitivity analysis as $0.001\% < m_p < 0.02\%$.

IV. AGGREGATED SINGLE-ORDER MODEL

Using the sensitivity analysis-based simplification method, the order of droop-based and PQ-controlled DGU models including the coupling line are reduced from 13 and 10 to 5 and 4, respectively. Moreover, the order of the case study MGs in Figs. 7(a) and 7(b) are reduced from 38 and 54 to 14 and 20, respectively. Although the low-frequency MG models are reduced well, the high-level dynamic studies, e.g. the frequency stability and control of IMGs justify the importance of finding a very low-order model.

As mentioned in Section III-B, the low-frequency dynamic behaviour of autonomous AC MGs can be summarized in the oscillatory DLFMs representing the interactions among DGUs and the base DGU. In fact, each DGU excluding the base DGU, whether droop-based or PQ-controlled, is equivalent to an oscillatory DLFM. Aggregating any number of the oscillatory DLFMs to one oscillatory mode leads to a low-frequency second-order model for autonomous AC MGs, which in turn results in a single-order frequency model.

This article has been accepted for publication in a future issue of this journal, but has not been fully edited. Content may change prior to final publication. Citation information: DOI 10.1109/TPWRS.2020.3040804, IEEE Transactions on Power Systems

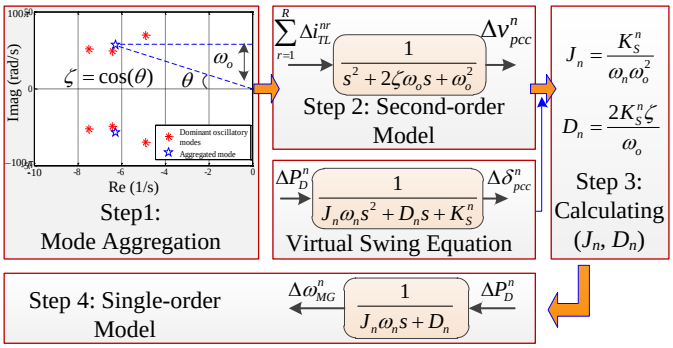

Fig. 9. Four-step method for calculating the single-order frequency model of autonomous AC microgrids.

Fig. 9 shows four steps for finding the proposed single-order model for autonomous AC MGs as follows:

- Step 1: Aggregate the dominant oscillatory modes obtained from the simplified low-frequency model presented in Section III.
- Step 2: Find the second-order model using the aggregated complex conjugate mode.
- Step 3: Calculate the virtual inertia and damping coefficient (J,D) by mapping the second-order model on the virtual swing equation.
- Step 4: Exclude the single-order frequency model for autonomous AC MGs from the second-order model.

A. Aggregation Method for Dominant Oscillatory Modes

Consider that k oscillatory DLFMs are obtained from the proposed simplified model presented in Section III as $\{\lambda^1_{DLFM}, ..., \lambda^{2k}_{DLFM}\}$, which can be represented by a state space model as

$$\dot{x} = Ax, \tag{9}$$

where $x \in R^{2k\times 1}$ and $A = diag\{\lambda^1_{DLFM}, ..., \lambda^{2k}_{DLFM}\}$. The goal is to find the state matrix F of the aggregated system as

$$\dot{z} = Fz, \tag{10}$$

where $z \in R^{l\times 1}$ is called the aggregation of x and they are correlated as $z(t) = Cx(t)$. $C \in R^{l\times 2k}, (l < 2k)$ is constant aggregation matrix of x. Finally, F can be calculated as follows [18]

$$F = CAC^{+}, \tag{11}$$

where C^+ is the pseudo-inverse of the non-square matrix C, which can be calculated as $C^+ = C^T(CC^T)^{-1}$.

Since all oscillatory DLFMs are interested to be aggregated as one oscillatory mode, z is a 2×1 vector comprising a pair of complex conjugate eigenvalues. Thus one can find a second-order transfer function for each autonomous AC MG as follows

$$G_{MG}(s) = \frac{1}{s^2 + 2\zeta\omega_0 s + \omega_0^2}, \tag{12}$$

where ζ and ω_0 are the damping ratio and undamped natural frequency of the aggregated model. The input and output of the transfer function can be determined according to the details of the simplified MG model. Based on the models presented in Fig. 6 for droop-based and PQ-controlled DGUs, the simplified model of each DGU can be represented as

$$\Delta i^{DGU}_{odq} = G^{DGU}_{com}(s)\Delta\omega_{com} + G^{DGU}_{pcc}(s)\Delta v^n_{pcc,dq}, \tag{13}$$

where $G^{DGU}_{com}(s)$ and $G^{DGU}_{pcc}(s)$ can be calculated employing the interconnection method [29]. By applying KCL for the PCC in Fig. 2, $\Delta v^n_{pcc,dq}$ is obtained as follows

$$\Delta v^n_{pcc,dq} = R_v \sum_{s=1}^{S} \Delta i^{DGU_s}_{odq} + R_v \sum_{r=1}^{R} \Delta i^{nr}_{TL,dq} - R_v \Delta i_{Lo,dq}, \tag{14}$$

where R_v is the virtual resistor [12], [29]. Substituting (13) and the static model of integrated load in (14), all DGU currents are aggregated at the PCC and $\Delta v^n_{pcc,dq}$ can be indicated as

$$\Delta v^n_{pcc,dq} = G^{pcc}_{IL}(s) \sum_{r=1}^{R} \Delta i^{nr}_{TL,dq}, \tag{15}$$

where $G^{pcc}_{IL}(s)$ can also be calculated using the interconnection method [29]. Therefore, $\sum_{r=1}^{R} \Delta i^{nr}_{TL,dq}$ and $\Delta v^n_{pcc,dq}$ are the input and output of the second-order model of MG$_n$ (12).

B. Virtual Swing Equation-Based Single-Order Model

Here, a virtual swing equation is considered for fully inverter-based autonomous AC MGs as

$$J_n\omega_n \frac{d\Delta\omega^n_{MG}}{dt} = \Delta P^n_{MG} - D_n\Delta\omega^n_{MG}, \tag{16}$$

where J_n and D_n are the virtual moment of inertia and damping coefficient of MG$_n$. ΔP^n_{MG} is the net value of input MG$_n$ power as

$$\Delta P^n_{MG} = \sum_{q=1}^{Q} T_{qn}(\Delta\delta^q_{pcc} - \Delta\delta^n_{pcc}), \tag{17}$$

where $\Delta\delta^q_{pcc}$ is the PCC voltage angle of interconnected MG$_q$ to the studied MG$_n$ and T_{qn} can be calculated as

$$T_{qn} = \frac{V^q_{pcc}V^n_{pcc}}{Z^2_{qn}}[R_{qn}\sin(\Delta\delta^{qn}_{pcc}) + X_{qn}\cos(\Delta\delta^{qn}_{pcc})], \tag{18}$$

where $\Delta\delta^{qn}_{pcc} = \delta^q_{pcc} - \delta^n_{pcc}$, $Z_{qn} = \sqrt{R^2_{qn} + X^2_{qn}}$, R_{qn} and X_{qn} are the resistance and reactance of the tie-line between MG$_q$ and MG$_n$. Substituting (17) and $\Delta\omega^n_{MG} = d\Delta\delta^n_{pcc}/dt$ in (16) and taking Laplace transform results in

$$G^{MG_n}_{VSE}(s) = \frac{\Delta\delta^n_{pcc}(s)}{\Delta P^n_D(s)} = \frac{1}{J_n\omega_n s^2 + D_n s + K^n_S}, \tag{19}$$

where K^n_S and ΔP^n_D are the synchronizing power coefficient and disturbance power of MG$_n$ as

$$K^n_S = \sum_{q=1}^{Q} T_{qn}, \Delta P^n_D = \sum_{q=1}^{Q} T_{qn}\Delta\delta^q_{pcc}.$$

Note that the transfer functions (12) and (19) are equivalent. Therefore, each autonomous AC MG can be mapped on a

This article has been accepted for publication in a future issue of this journal, but has not been fully edited. Content may change prior to final publication. Citation information: DOI 10.1109/TPWRS.2020.3040804, IEEE Transactions on Power Systems

virtual swing equation, and J_n and D_n can be calculated by comparing (12) and (19), which results in

$$J_n = \frac{K_S^n}{\omega_n \omega_o^2}, D_n = \frac{2K_S^n \zeta}{\omega_o}. \quad (20)$$

At last, considering $\Delta\omega_{MG}^n = d\Delta\delta_{pcc}^n/dt$ and (19), the single-order frequency model of autonomous AC MG_n is as

$$G_{freq}^{MG_n}(s) = \frac{\Delta\omega_{MG}^n(s)}{\Delta P_D^n(s)} = \frac{1}{J_n\omega_n s + D_n}. \quad (21)$$

V. Use of the Single-Order Model in Frequency Control of Interconnected Microgrids

The proposed single-order model facilitates the high-level control studies of large-scale IMGs, e.g. the frequency control. Fig. 10(a) shows three different autonomous AC MGs interconnected through three tie-lines. The frequency and tie-line power control among the MGs are done in the secondary control layer. Fig. 10(b) shows the frequency model of MG_1 within the studied three IMGs including the single-order model of MG_1, tie-line power (ΔP_{TL1}) model [39] and the secondary controller. The frequency model of MG_2 and MG_3 is similar to the MG_1 frequency model with individual parameters. In Fig. 10(b), β_1 is the MG_1 frequency bias calculated as

$$\beta_1 = \sum_{i=1}^{m} (1/m_p^i) + D_{L1}, \quad (22)$$

where m_p^i is the $\omega - P$ droop gain of DER_i and D_{L1} is the damping coefficient of the MG_1 load.

The secondary controller is selected as being a PI type. In order to design the secondary controllers, the sequential loop closing method [40] is used, such that MG_1 controller is tuned using PID tuning block in MATLAB/SIMULINK when MG_2 and MG_3 control loops are open. Then MG_2 controller is tuned and finally MG_3 control loop is closed to tune its controller. Note that in this method, the first loop is closed independent to the other loops. Nevertheless, during closing next loops and design the corresponding PI controllers, the previous loops are closed and their interactions are considered in the design process. Hence, the frequency control is done uniformly. In order to consider the interactions simultaneously among the three control loops, the centralized methods of multivariable control systems [41] can be employed as future works.

VI. Simulation Results

The frequency stability and dynamics of three IMGs shown in Fig. 10(a) are studied to introduce the inter-MG DLFMs and show a stable operation of the secondary controllers designed in Section V. All the MGs are of low-voltage AC type, which have the same nominal frequency and voltage as 50 Hz and 400 V. They have a general structure shown in Fig. 2, which MG_1 consists of four droop-based DGUs, MG_2 has two droop-based and one PQ-controlled DGUs, and MG_3 contains three droop-based and two PQ-controlled DGUs. The general data of the MG modules is presented in [42] and the parameters of the frequency IMG model shown in Fig. 10(b) are found by applying the four-step method introduced in Fig. 9 for the three MGs, which are indicated in Table III. Finally, Fig. 10(c) shows the low-order frequency model of the studied three IMGs. Note that each box indicates the low-order frequency model of each MG, e.g. the contents of MG_1 box is shown in Fig. 10(b) within red dashed outline. The frequency interactions of the MGs is exhibited in Fig. 10(c).

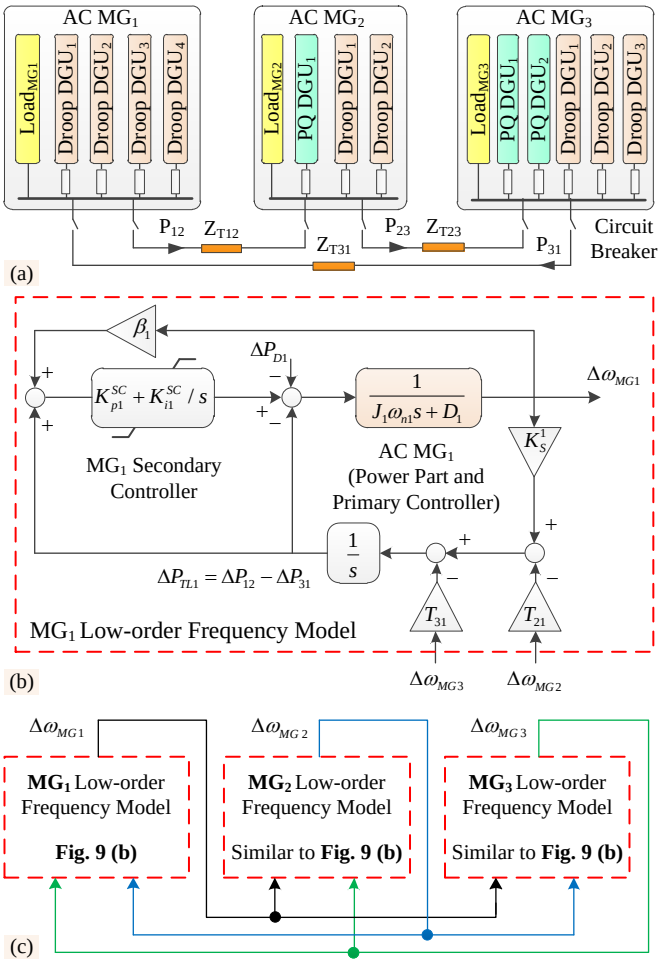

Fig. 10. Case study for frequency control: (a) Three interconnected AC microgrids through circuit breakers and tie-lines, (b) low-order frequency model of MG_1 including the single-order model, controller, and tie-line power, (c) low-order frequency model of the studied system.

TABLE III. Calculated Parameters of The IMGs in Fig. 10

	D $(\frac{kW.s}{rad})$	J $(\frac{W.s^2}{rad})$	β $(\frac{kW.s}{rad})$	T_{gn} $(\frac{10^5 W}{rad})$	K_p^{SC}	K_i^{SC}
MG_1	5.6	1.45	7	$T_{21}=1.4$ $T_{31}=2.3$	0	-9.16
MG_2	1.9	0.71	1.9	$T_{12}=1.4$ $T_{32}=0.9$	0	-4.71
MG_3	3.8	1.4	3.8	$T_{13}=2.3$ $T_{23}=0.9$	0	-8.98

A. Inter-Microgrid Oscillatory Modes

The participation matrix of the state space model of the three IMGs shown in Fig. 10, can be seen in Fig. 11. SOM, SC, and Int indicate the state variables of the single-order MG model, secondary PI controller, and the integrator modeling tie-line power dynamics, respectively. The contribution of each state variable in each eigenvalue is calculated and then normalized using the corresponding relationships in [43]. The participation

This article has been accepted for publication in a future issue of this journal, but has not been fully edited. Content may change prior to final publication. Citation information: DOI 10.1109/TPWRS.2020.3040804, IEEE Transactions on Power Systems

	-1.74 ± j38.26		-1.10 ± j35.24		-5.35 ± j8.24		-8.48	-4.87	0
	λ_1	λ_2	λ_3	λ_4	λ_5	λ_6	λ_7	λ_8	λ_9
SOM_{MG1}	0.26	0.26	0.03	0.03	0.17	0.17	0.02	0.01	0
SC_1	0.06	0.06	0.01	0.01	0.20	0.20	0.35	0.02	0
Int_1	0.24	0.24	0.03	0.03	0.06	0.06	0.03	0.02	0.55
SOM_{MG2}	0.15	0.15	0.21	0.21	0.10	0.10	0	0.03	0
SC_2	0.02	0.02	0.03	0.03	0.05	0.05	0	0.84	0
Int_2	0.15	0.15	0.20	0.20	0.05	0.05	0	0.03	0.15
SOM_{MG3}	0.05	0.05	0.23	0.23	0.16	0.16	0.03	0.01	0
SC_3	0.01	0.01	0.06	0.06	0.16	0.16	0.53	0.01	0
Int_3	0.05	0.05	0.22	0.22	0.03	0.03	0.03	0.02	0.3
	Interaction between MG_1 and MG_2		Interaction between MG_2 and MG_3		Interaction among all three MGs		Dynamic modes of secondary controllers		Integrators mode

Fig. 11. Participation Matrix of the studied three interconnected AC microgrids shown in Fig. 10.

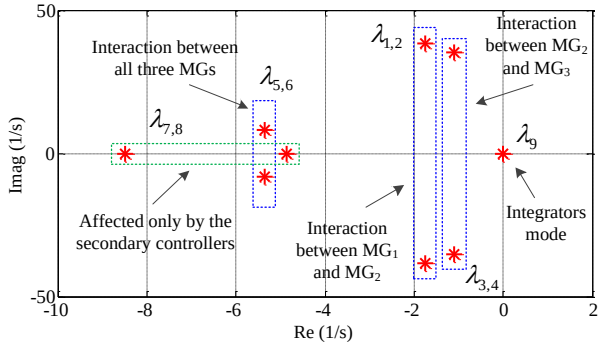

Fig. 12. Eigenvalues of the studied three interconnected AC microgrids shown in Fig. 10.

matrix results are also shown in Fig. 12 by the qualitative interpretations added to the nine eigenvalues of the 3-IMGs. λ_1-λ_6 are the main inter-MG modes affected by all modules including the inner MG models, the secondary controllers, and the tie-line power values. According to the larger participation factors of each dynamic mode, i.e. column data of the participation matrix shown in Fig. 11, $\lambda_{1,2}$, $\lambda_{3,4}$, and $\lambda_{5,6}$ show the interaction between MG_1 and MG_2, the interaction between MG_2 and MG_3, and the interaction between all three MGs, respectively. $\lambda_{7,8}$ are the non-oscillatory modes affected only by the secondary controllers and λ_9 is a non-critical zero mode due to the tie-line power integrators.

Note that the main inter-MG modes are oscillatory, which may cause the frequency oscillation and instability, especially considering the low inertia of IMGs. The possible frequency instability and even the frequency fluctuations can be confronted by designing the secondary controller based on the behaviour of inter-MG modes.

B. Frequency Response

The frequency response of the MGs is shown in Fig. 13. Three load changes as +18 %, -18 %, and +23 % of the rated controllable power for frequency control (sum of droop-based DGU powers) are applied as ΔP_D in MG_1, MG_2, and MG_3, respectively. Generally, the dynamics of three MG frequencies are similar due to interlinking using circuit breakers, i.e. the power section of IMGs is uniformed unlike interconnection using back-to-back converters [4], [5], [29]. Moreover, the frequency oscillations can be seen, which are caused by the inter-MG modes. Nevertheless, there are differences in the

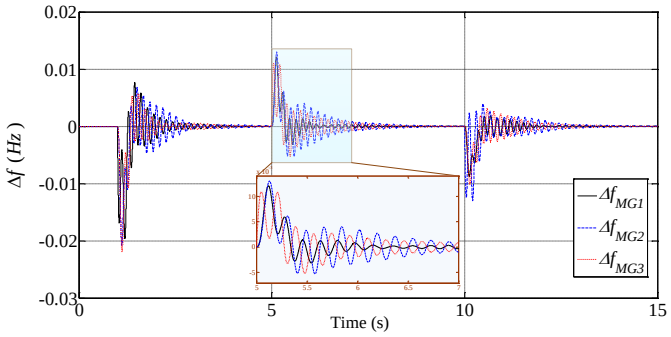

Fig. 13. Frequency response of the studied three interconnected AC microgrids. MG_1 load increase as 18 % rated controllable power at $t = 1$ s, MG_3 load decrease as 18 % rated controllable power at $t = 10$ s, MG_2 load increase as 23 % rated controllable power at $t = 20$ s.

transients, e.g. nadir and rate of change of frequency due to the different amounts of virtual J and D. It can be seen that the frequency stability is guaranteed against several small disturbances by the secondary PI controllers.

It is noteworthy to remind that the proposed IMG model is a small-signal type, which cannot be used to investigate the system behavior during large disturbances, e.g. DER/MG disconnection, or inner nonlinear phenomena, e.g. limiter saturation of converter controllers. Furthermore, the fast and medium speed dynamics are removed. Therefore, the corresponding variables studies cannot be done using the proposed model, e.g. the voltage stability analysis.

C. Comparison between Using Detailed and Single-order Models

Fig. 14 shows a comparison between two different models of the studied IMGs including Model 1 with the detailed MG_1 model and the single-order models of MG_2 and MG_3, and Model 2 with the single-order models of all the three MGs shown in Fig. 10(c). According to the DLFMs, it is easy to understand that Model 2 is a simplified type of Model 1 after the perturbation and aggregation processes. Fig. 15 shows the frequency response of Model 1 for 18 % MG_1 load increase with respect to its rated controllable power at t=0 s. The characteristics like overshoot and oscillation damping are not fully similar to the frequency response of Model 1 shown in Fig. 13 due to two reasons. The first reason is the difference between the detailed and simplified models of MG_1 in medium and high frequencies. On the other hand, the stabilizing parameter ranges of the MG_1 secondary controller are different in Model 1 and Model 2. Therefore, the secondary controller parameters, which are obtained by the sequential loop closing, are different for the models. In Model 1, the K_p^{SC} is 0 for all three MGs like Model 2, however the K_i^{SC} is as -3.11, -4.71, and -8.98, respectively.

The important point is the simulation time duration of the frequency response. The simulation time of Model 2 is selected as 30 s as shown in Fig. 13, which is executed less than 3 real seconds. Nevertheless, the simulation time of Model 1 is selected as 3 s, which is executed in 510 real seconds using the same processor Intel Core i7-7500U, 2.7 GHz with Turbo boost up to 3.5 GHz. In other words, for the same simulation

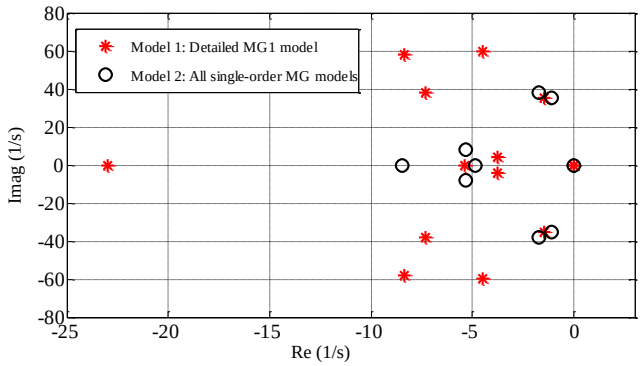

Fig. 14. The comparison between two models of the studied IMGs including Model 1 with detailed MG_1 model and single-order model of MG_2 and MG_3, Model 2 with single-order model of the all three MGs.

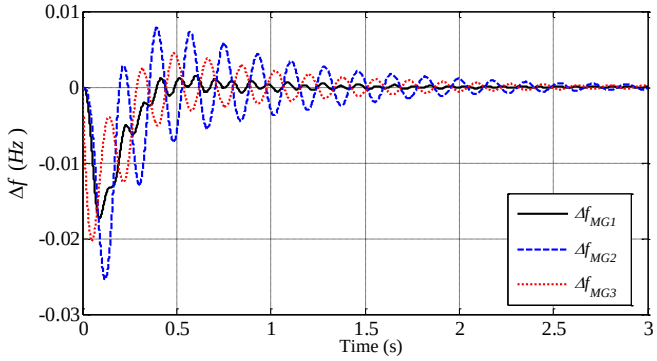

Fig. 15. Frequency response of Model 1 when MG_1 load increase as 18 % rated controllable power at $t = 0$ s.

time of both the models, e.g. 30 s, the required real time for Model 1 is as $5100/3 = 1700$ times of the required real time for Model 2. Therefore, using the detailed MG model is hard and time-consuming to study the IMG dynamics, especially for a large number of IMGs. In contrast, very low simulation time duration is a significant feature for the low-order frequency model of the IMGs.

VII. Conclusion

In this paper, two reduced order models are proposed for autonomous AC microgrid analysis. The first one is the sensitivity analysis-based simplification method in which singular and regular perturbation methods are employed to reduce the simplified model order to less than half of the detailed model order. This low-order model is useful to study slow dynamics and design medium-level controllers of islanded AC microgrids, e.g. the secondary controller. The second model is the single-order frequency model obtained by aggregating the low-order model and using the virtual swing equation concept. This model is applicable for the high-level control studies of large-scale interconnected microgrids, where the detailed and even low-order models lead to very large-order models, which make the analysis and synthesis difficult. The frequency analysis of the typical three interconnected microgrids shows the inter-microgrid modes expressing the interactions among the microgrid frequencies, which cause the frequency oscillations and may lead to the instability or protection devices trip.

References

[1] Q. Shafiee, T. Dragičević, J. C. Vasquez, and J. M. Guerrero, "Hierarchical control for multiple dc-microgrids clusters," *IEEE Trans. Energy Conv.*, vol. 29, no. 4, pp. 922–933, 2014.

[2] J. Zhou and et al., "Event-based distributed active power sharing control for interconnected ac and dc microgrids," *IEEE Trans. Smart Grid*, vol. 5, no. 6, pp. 6815–6828, 2018.

[3] E. Pashajavid, A. Ghosh, and F. Zare, "A multimode supervisory control scheme for coupling remote droop-regulated microgrids," *IEEE Trans. Smart Grid*, vol. 9, no. 5, pp. 5381–5392, 2018.

[4] M. Naderi, Y. Khayat, Q. Shafiee, T. Dragicevic, H. Bevrani, and F. Blaabjerg, "Interconnected autonomous ac microgrids via back-to-back converters-part II: Stability analysis," *IEEE Trans. Power Electron.*, vol. 35, no. 11, pp. 11 801–11 812, 2020.

[5] R. Zamora and A. K. Srivastava, "Multi-layer architecture for voltage and frequency control in networked microgrids," *IEEE Trans. Smart Grid*, vol. 9, no. 3, pp. 2076–2085, 2018.

[6] Y. Zhang, L. Xie, and Q. Ding, "Interactive control of coupled microgrids for guaranteed system-wide small signal stability," *IEEE Trans. Smart Grid*, vol. 7, no. 2, pp. 1088–1096, 2016.

[7] M. Fathi and h. Bevrani, "Adaptive energy consumption scheduling for connected microgrids under demand uncertainty," *IEEE Trans. Power Del.*, vol. 28, no. 3, pp. 1576–1583, 2013.

[8] I. U. Nutkani, P. C. Loh, and F. Blaabjerg, "Distributed operation of interlinked ac microgrids with dynamic active and reactive power tuning," *IEEE trans. ind. appl.*, vol. 49, no. 5, pp. 2188–2196, 2013.

[9] R. Majumder and G. Bag, "Parallel operation of converter interfaced multiple microgrids," *Int. J. Electr. Power & Energy Syst.*, vol. 55, pp. 486–496, 2014.

[10] C. Schwaegerl, L. Tao, J. P. Lopes, A. Madureira, P. Mancarella, A. Anastasiadis, N. Hatziargyriou, and A. Krkoleva, "Advanced architectures and control concepts for more microgrids," *Siemens AG*, no. SES6-019864, 2009.

[11] H. Bevrani, B. François, and T. Ise, *Microgrid dynamics and control*. John Wiley & Sons, 2017, Hoboken, NJ, USA.

[12] N. Pogaku, M. Prodanovic, and T. C. Green, "Modeling, analysis and testing of autonomous operation of an inverter-based microgrid," *IEEE Trans. Power Electron.*, vol. 22, no. 2, pp. 613–625, 2007.

[13] L. Luo and S. V. Dhople, "Spatiotemporal model reduction of inverter-based islanded microgrids," *IEEE Trans. Energy Conv.*, vol. 29, no. 4, pp. 823–832, 2014.

[14] V. Mariani, F. Vasca, J. C. Vásquez, and J. M. Guerrero, "Model order reductions for stability analysis of islanded microgrids with droop control," *IEEE Trans. Ind. Electron.*, vol. 62, no. 7, pp. 4344–4354, 2014.

[15] M. Rasheduzzaman, J. A. Mueller, and J. W. Kimball, "Reduced-order small-signal model of microgrid systems," *IEEE Trans. Sustainable Energy*, vol. 6, no. 4, pp. 1292–1305, 2015.

[16] P. Vorobev, P.-H. Huang, M. Al Hosani, J. L. Kirtley, and K. Turitsyn, "High-fidelity model order reduction for microgrids stability assessment," *IEEE Trans. Power Syst.*, vol. 33, no. 1, pp. 874–887, 2017.

[17] I. P. Nikolakakos, H. Zeineldin, M. S. El-Moursi, and J. L. Kirtley, "Reduced-order model for inter-inverter oscillations in islanded droop-controlled microgrids," *IEEE Trans. Smart Grid*, vol. 9, no. 5, pp. 4953–4963, 2017.

[18] M. Jamshidi, *Large-scale systems: modeling, control, and fuzzy logic*. Prentice-Hall, Inc., 1996.

[19] A. Adib, F. Fateh, M. B. Shadmand, and B. Mirafzal, "A reduced-order technique for stability investigation of voltage source inverters," in *IEEE Energy Conv. Cong. and Exposition (ECCE)*, 2018, pp. 5351–5356.

[20] I. P. Nikolakakos and et al., "Stability evaluation of interconnected multi-inverter microgrids through critical clusters," *IEEE Trans. Power Syst.*, vol. 31, no. 4, pp. 3060–3072, 2016.

[21] Z. Shuai and et al., "Dynamic equivalent modeling for multi-microgrid based on structure preservation method," *IEEE Trans. Smart Grid*, vol. 10, no. 4, pp. 3929–3942, 2018.

[22] F. TP462, "Identification of electromechanical modes in power systems," *IEEE Task Force Report*, 2012.

[23] P. W. Sauer, M. A. Pai, and J. H. Chow, *Power system dynamics and stability: with synchrophasor measurement and power system toolbox*. John Wiley & Sons, 2017.

[24] H. Bevrani, M. Watanabe, and Y. Mitani, *Power System Monitoring and Control*. John Wiley & Sons, 2014.

[25] E. O. Kontis, T. A. Papadopoulos, A. I. Chrysochos, and G. K. Papagiannis, "Measurement-based dynamic load modeling using the

vector fitting technique," *IEEE Trans. Power Syst.*, vol. 33, no. 1, pp. 338–351, 2017.
[26] C. Lu, "Wavelet fuzzy neural networks for identification and predictive control of dynamic systems," *IEEE Trans. Ind. Electron.*, vol. 58, no. 7, pp. 3046–3058, 2010.
[27] E. O. Kontis, T. A. Papadopoulos, M. H. Syed, E. Guillo-Sansano, G. M. Burt, and G. K. Papagiannis, "Artificial-intelligence method for the derivation of generic aggregated dynamic equivalent models," *IEEE Trans. Power Syst.*, vol. 34, no. 4, pp. 2947–2956, 2019.
[28] Z. Zhao, P. Yang, Y. Wang, Z. Xu, and J. M. Guerrero, "Dynamic characteristics analysis and stabilization of pv-based multiple microgrid clusters," *IEEE Trans. Smart Grid*, vol. 10, no. 1, pp. 805–818, 2017.
[29] M. Naderi, Y. Khayat, Q. Shafiee, T. Dragicevic, H. Bevrani, and F. Blaabjerg, "Interconnected autonomous ac microgrids via back-to-back converters—part I: small-signal modeling," *IEEE Trans. Power Electron.*, vol. 35, no. 5, pp. 4728 – 4740, 2020.
[30] Z. Yuan, Z. Du, C. Li, and T. An, "Dynamic equivalent model of vsc based on singular perturbation," *IET Generation, Transmission & Distribution*, vol. 10, no. 14, pp. 3413–3422, 2016.
[31] X. Guo, Z. Lu, B. Wang, X. Sun, L. Wang, and J. M. Guerrero, "Dynamic phasors-based modeling and stability analysis of droop-controlled inverters for microgrid applications," *IEEE Trans. Smart Grid*, vol. 5, no. 6, pp. 2980–2987, 2014.
[32] C. Wang, H. Yu, P. Li, J. Wu, and C. Ding, "Model order reduction for transient simulation of active distribution networks," *IET Generation, Transmission & Distribution*, vol. 9, no. 5, pp. 457–467, 2015.
[33] E. A. A. Coelho, P. C. Cortizo, and P. F. D. Garcia, "Small-signal stability for parallel-connected inverters in stand-alone ac supply systems," *IEEE Trans. Ind. Appl.*, vol. 38, no. 2, pp. 533–542, 2002.
[34] H. Golpîra, H. Seifi, A. R. Messina, and M.-R. Haghifam, "Maximum penetration level of micro-grids in large-scale power systems: frequency stability viewpoint," *IEEE Trans. Power Sys.*, vol. 31, no. 6, pp. 5163–5171, 2016.
[35] H. Golpîra, H. Seifi, and M. R. Haghifam, "Dynamic equivalencing of an active distribution network for large-scale power system frequency stability studies," *IET Gen., Transm. & Dist.*, vol. 9, no. 15, pp. 2245–2254, 2015.
[36] M. Gheisarnejad and M. H. Khooban, "Secondary load frequency control for multi-microgrids: Hil real-time simulation," *Soft Computing*, vol. 23, no. 14, pp. 5785–5798, 2019.
[37] A. H. Chowdhury and M. Asaduz-Zaman, "Load frequency control of multi-microgrid using energy storage system," in *8th IEEE Int. conf. Electr. and Computer Eng.*, 2014, pp. 548–551.
[38] Y. Khayat and et al., "Decentralized optimal frequency control in autonomous microgrids," *IEEE Trans. Power Syst.*, vol. 34, no. 3, pp. 2345–2353, 2018.
[39] H. Bevrani, "Robust power system frequency control," Springer, 2014.
[40] U. Ubaid, S. Daley, and S. Pope, "Design of remotely located and multi-loop vibration controllers using a sequential loop closing approach," *Control Eng. Pract.*, vol. 38, pp. 1–10, 2015.
[41] P. Albertos and S. Antonio, *Multivariable control systems: an engineering approach*. Springer Science & Business Media, 2006.
[42] M. Naderi, Y. Khayat, Q. Shafiee, T. Dragicevic, F. Blaabjerg, and H. Bevrani, "An emergency active and reactive power exchange solution for interconnected microgrids," *J. Emerging and Sel. Topics Power Electron.*, 2019, DOI: 10.1109/JESTPE.2019.2954113.
[43] M. Naderi and et al., "Model validation of power electronics-based networked micro-grids by prony analysis," in *21st Euro. Conf. Power Electron. and Appl.* IEEE, Sept. 2019, pp. 1–9.

Mobin Naderi (S'16) received the B.Sc., M.Sc. and Ph.D. degrees in Electrical Engineering from Tabriz University, Tabriz, Iran, Iran University of Science and Technology, Tehran, Iran, and University of Kurdistan, Sanandaj, Iran, respectively in 2012, 2014, and 2019. He was a Visiting PhD student with Department of Energy Technology, Aalborg University, Aalborg, Denmark. He is now a post-doctoral researcher at University of Kurdistan, Iran. His research interests focus on modeling, stability analysis and control of autonomous/interconnected microgrids, and robust control methods.

Qobad Shafiee (S'13–M'15–SM'17) received PhD degree in Electrical Engineering from the Department of Energy Technology, Aalborg University (Denmark) in 2014. He is currently an Assistant Professor, Director of International Affairs, and Co-Leader of the Smart/Micro Grids Research Center at the University of Kurdistan (Sanandaj, Iran), where he was a lecturer from 2007 to 2011. In 2014, he was a Visiting Scholar with the Electrical Engineering Department, the University of Texas at Arlington, Arlington, TX, USA. He was a Post-Doctoral Fellow with the Department of Energy Technology, Aalborg University in 2015. His current research interests include modeling, energy management, control of power electronics-based systems and microgrids, and model predictive and optimal control of modern power systems.

Frede Blaabjerg (S'86–M'88–SM'97–F'03) was with ABB-Scandia, Randers, Denmark, from 1987 to 1988. From 1988 to 1992, he got the PhD degree in Electrical Engineering at Aalborg University in 1995. He became an Assistant Professor in 1992, an Associate Professor in 1996, and a Full Professor of power electronics and drives in 1998. From 2017 he became a Villum Investigator. He is honoris causa at University Politehnica Timisoara (UPT), Romania and Tallinn Technical University (TTU) in Estonia.

His current research interests include power electronics and its applications such as in wind turbines, PV systems, reliability, harmonics and adjustable speed drives. He has published more than 600 journal papers in the fields of power electronics and its applications. He is the co-author of four monographs and editor of ten books in power electronics and its applications.

He has received 32 IEEE Prize Paper Awards, the IEEE PELS Distinguished Service Award in 2009, the EPE-PEMC Council Award in 2010, the IEEE William E. Newell Power Electronics Award 2014, the Villum Kann Rasmussen Research Award 2014 and the Global Energy Prize in 2019. He was the Editor-in-Chief of the IEEE TRANSACTIONS ON POWER ELECTRONICS from 2006 to 2012. He has been Distinguished Lecturer for the IEEE Power Electronics Society from 2005 to 2007 and for the IEEE Industry Applications Society from 2010 to 2011 as well as 2017 to 2018. In 2019-2020 he serves a President of IEEE Power Electronics Society. He is Vice-President of the Danish Academy of Technical Sciences too. He is nominated in 2014-2018 by Thomson Reuters to be between the most 250 cited researchers in Engineering in the world.

Hassan Bevrani (S'90 - M'04 - SM'08) received PhD degree in electrical engineering from Osaka University (Japan) in 2004. Currently, he is a full professor and the Program Leader of Smart/Micro Grids Research Center (SMGRC) at the University of Kurdistan (UOK). From 2016 to 2019 he was the UOK vice-chancellor for research and technology. Over the years, he has worked as senior research fellow and visiting professor with Osaka University, Kumamoto University (Japan), Queensland University of Technology (Australia), Kyushu Institute of Technology (Japan), Centrale Lille (France), and Technical University of Berlin (Germany). Prof. Bevrani is the author of 6 international books, 15 book chapters, and more than 300 journal/conference papers. His current research interests include smart grid operation and control, power systems stability and optimization, Microgrid dynamics and control, and Intelligent/robust control applications in power electric industry.